Journal of Alloys and Compounds 509 (2011) 4935–4939

Contents lists available at ScienceDirect

Journal of Alloys and Compounds

journal homepage: www.elsevier.com/locate/jallcom

Optical and thermal properties of P_2O_5–Na_2O–CaO–Al_2O_3:CoO glasses doped with transition metals

S. Cetinkaya Colak*, E. Aral

Eskisehir Osmangazi University, Department of Physics, 26480 Eskisehir, Turkey

ARTICLE INFO

Article history:
Received 12 October 2010
Received in revised form 25 January 2011
Accepted 30 January 2011
Available online 24 February 2011

Keywords:
Oxide glasses
Optical properties
Thermal conductivity
Solar collectors

ABSTRACT

The aim of this paper is to report the optical and thermal properties of V_2O_5 and CuO doped P_2O_5–Na_2O–CaO–Al_2O_3:CoO glasses so as to investigate their possible use in solar collection applications. The optical absorption spectra of the glasses at room temperature were in the spectral range of 200–1100 nm. The optical band gaps of the glass samples were determined for direct and indirect transitions. When transition metal ions doped to the base glass, the optical band gap decreased. Changes in the refractive indices vs. wavelength for all the specimens were also examined by spectroscopic ellipsometry. By measuring the heat capacities and thermal diffusion coefficients of the specimens at varying temperatures, their thermal conductivities were calculated to be in the 320–620 K temperature range. The obtained glasses seem to be promising materials and can be used in solar collector applications.

1. Introduction

Glass is used in a wide variety of fields, such as in electrical devices and building materials. Thermal conductivity is one of the principal properties considered during the manufacture and use of glass products. Due to their unique physical properties of having high thermal expansion coefficients, low melting and softening temperatures, high electrical conductivity, ultraviolet (UV) transmission, and optical characteristics, phosphate glasses, of all the oxide glasses produced, are generally considered to be both scientifically and technologically important materials [1–5]. These glasses are known for having lower glass transition temperatures and have attracted considerable interest in recent years because of their potential for technological applications, particularly in optics [6], and even more so in laser systems and biomaterials research [7,8].

Of particular interest are glasses with high concentrations of transition metals owing to both their semiconducting properties [9–13] and their optical absorption in the visible range, resulting in coloration of the glass states [14]. Glasses doped with transition metals also attract much attention because of their ability to memorize and photoconduct [15–17]. Moreover, they have the potential to be used in such applications as solid-state lasers [18], luminescent solar energy concentrators, and optical fibers for communication devices [19–23].

When considering the most appropriate transition metal ions for these purposes, vanadium and copper ions stand out as being the simplest and best-suited since they are characterized by a partially filled d shell which can exist in at least two valence states. Each of these valence states has a different electronic structure and coordination geometry [24].

Absorption spectroscopy is a valuable tool in the examination of materials. Just a cursory view of the absorption vs. the wavelength and the absorption edge is enough to reveal whether the material under investigation is crystalline or amorphous in nature. The absorption edge is very sharp in crystalline substances whereas it has a finite slope in amorphous substances.

This technique can also provide information about the optically induced transitions, the band structure, and the band gap of materials [25]. Variation in the optical band gap of phosphate glasses has previously been studied as a function of composition [26,27].

In this study, black glass was produced by CoO incorporation at high ratio into P_2O_5–Na_2O–CaO–Al_2O_3 glass structures. The effect of the transition metal ions V_2O_5 and CuO on the optical and thermal characteristics of black glass was then investigated.

2. Experimental

2.1. Glass preparation

Glass samples were prepared by the melt quench technique, and their starting batch compositions are listed in Table 1.

Appropriate amounts (all in weight %) of the reagent grade P_2O_5, Na_2CO_3, CaO, Al_2O_3, Co_3O_4 V_2O_5 and CuO powders were methodically weighed and thoroughly mixed. They were then melted in a thick-walled platinum crucible in the electric furnace for 2 h at 1573 K until a bubble free liquid was formed. The resultant melt

* Corresponding author. Tel.: +90 222 2393750x2827; fax: +90 222 2393578.
E-mail address: sccolak@ogu.edu.tr (S.C. Colak).

0925-8388/$ – see front matter © 2011 Elsevier B.V. All rights reserved.
doi:10.1016/j.jallcom.2011.01.172

Table 1
Compositions of glass structures (in wt%) studied in the present work.

Glass code	Glass structure
P1	%60 P_2O_5 + %20 Na_2O + %18 CaO + %2 Al_2O_3 (base glass)
P2	Base glass + %20 CoO (black glass)
P3	Black glass + %0.5 V_2O_5
P4	Black glass + %1 V_2O_5
P5	Black glass + %0.5 CuO
P6	Black glass + %1 CuO

was then poured into a graphite mould and subsequently annealed at 723 K for 1 h, then cooled slowly to room temperature.

2.2. Characterization tools

The amorphous state of the glasses was verified by X-ray powder diffraction patterns recorded in the 2θ range from 10° to 70° on a XRD-Rigaku Rint 2000 diffractometer using CuK_α radiation. The optical absorption spectra of the glasses at room temperature were recorded in the wavelength range of 200–1100 nm via Perkin Elmer Lambda 2S UV/VIS Spectrophotometer. The refractive index was determined over the wavelength range 300–900 nm by SC620 Spectroscopic Ellipsometer using the Lorentz model, which is better suited to describe the optical properties of layers that absorb light in a region of the measured spectral range [28,29]. Thermal diffusivity measurements were taken by using the laser flash technique. The measurements were captured with NETZSCH LFA 457 MicroFlash, and the specific heat capacity was measured by a differential scanning calorimeter (NETZSCH DSC409 PG) at temperature range from 320 to 620 K. Glass densities (ρ) were measured at room temperature using the Archimedes method with ethanol as the immersion fluid.

3. Results and discussion

3.1. Optical investigations

Fig. 1 shows the optical absorption spectra of all glasses against the wavelength 200–1100 nm. While absorption is observable only in the UV region of base glass, absorption was observed in both the visible and NIR regions when we incorporated 20% of CoO (P2) to the glass. By adding V_2O_5 into the named P2, a strong absorption occurs at the UV edge while CuO addition into the glass structure causes a strong absorption in the NIR region. V_2O_5 doping causes absorption in the 350–400 nm wavelength range. This is probably related to the V^{3+} ions present, which have a characteristic UV absorption at 350–400 nm. The absorption peak at 420 nm is almost certainly related to the vanadly tetravalent ions established by Ref. [30]. When the doping rate of V_2O_5 was increased (at 1%), this caused the absorption peak at 420 nm to have a little higher absorbance value than P3 glass (at 0.5%). When the amount of V_2O_5 was increased, it caused an increase in the number of vanadly tetravalent ions. Furthermore, when CuO doping was increased, it caused an increase in the absorbance value in the ~700–800 nm wavelength range. This

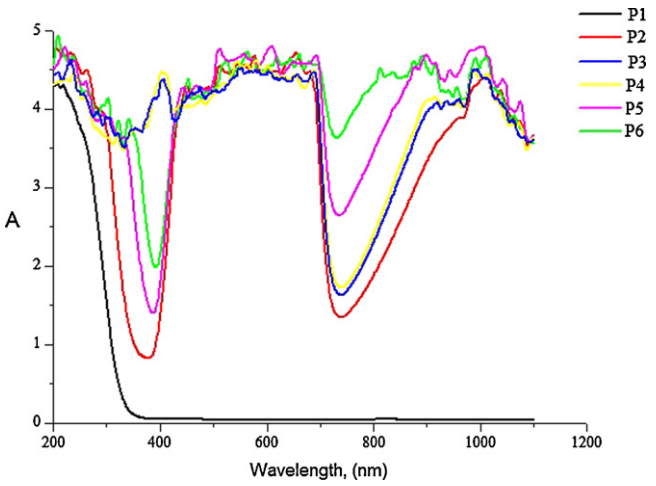

Fig. 1. Optical absorption spectra of all glasses.

Table 2
Direct, indirect band gap, refractive index and density values of glasses.

Glass code	Direct band gap (eV)	Indirect band gap (eV)	n	ρ (g/cm^3)
P1	4	3.43	1.475	2.619
P2	3.84	3.08	1.601	2.906
P3	3.4	2.08	1.595	2.910
P4	3.21	1.7	1.589	2.917
P5	3.6	2.31	1.599	2.916
P6	3.7	2.52	1.586	2.924

can be attributed to the absorption of Cu^{2+} ions in the octahedral coordination as reported in [31].

We evaluated the optical band gap (E_{opt}) of the glasses from the observed absorption edges. It is customary to plot $(\alpha h\upsilon)^2$ as a function of photon energy ($h\upsilon$) in order to find the optical energy band gaps (E_{opt}) for direct transitions by using Davis and Mott relation [32]. This relation holds very well above the exponential tail where it shows linear behavior. The straight region in these curves is extrapolated to meet the x-axis ($h\upsilon$). The value of ($h\upsilon$) at the meeting point yields a direct measure of the optical band energy (E_{opt}). For indirect transitions, it is determined by plotting $(\alpha h\upsilon)^{1/2}$ as a function of ($h\upsilon$) [33]. Graphs (direct and indirect transitions) for only P1 glass are shown in Fig. 2.

The direct and indirect band gap values of all the glasses are given in Table 2. The glass with the highest direct and indirect band gap values is P1 glass. Black glass (P2), produced by the incorpora-

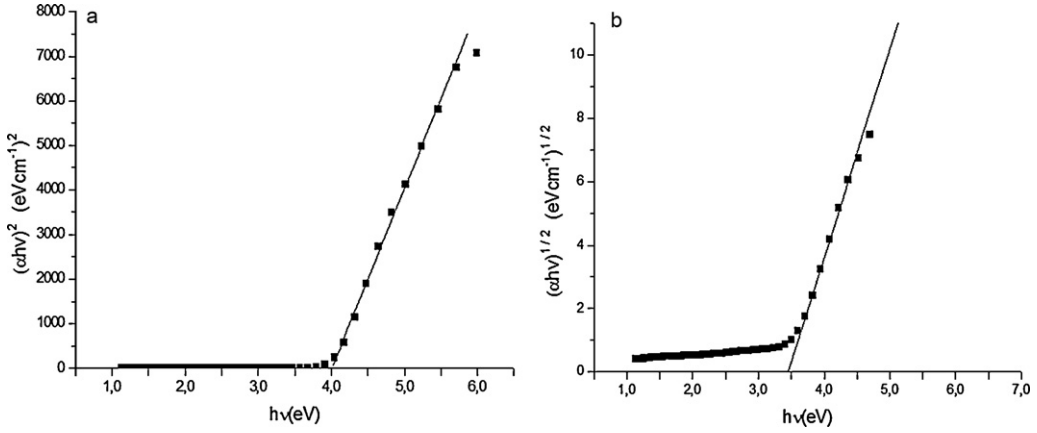

Fig. 2. The relation between (a) $(\alpha h\upsilon)^2$ and ($h\upsilon$) and (b) $(\alpha h\upsilon)^{1/2}$ and ($h\upsilon$) for P1 glass.

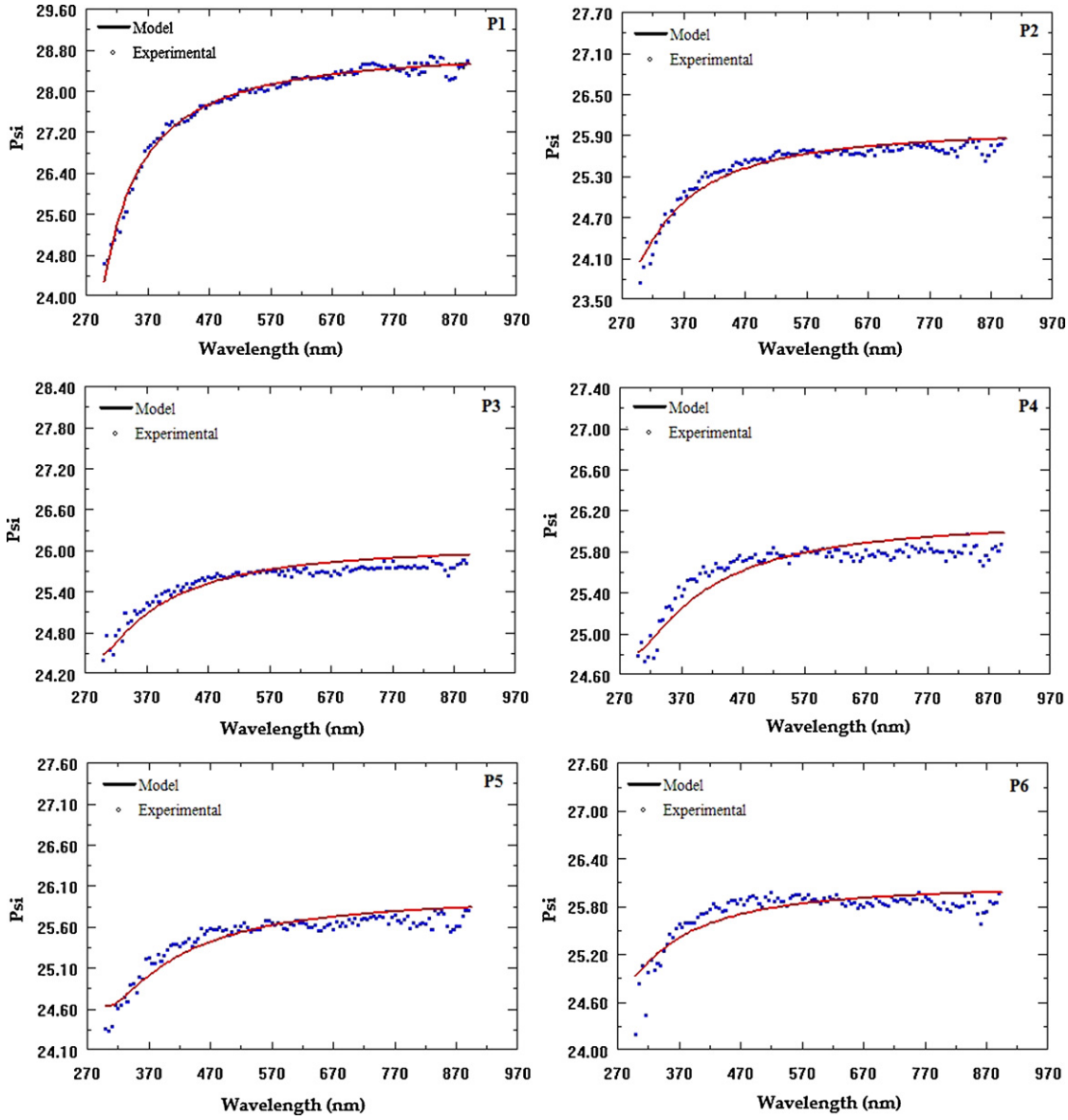

Fig. 3. SE spectra of glasses.

tion of 20% of CoO to the base glass, has a lower band gap than P1. V_2O_5 and CuO doping into the black glass lowered the band gap values. The lowest band gap values were determined for V_2O_5 doped glass structures.

In order to determine the refractive indices of the glasses, Ψ parameters were measured by using the polarization of the light reflected from the specimens in the ellipsometer device. These experimentally measured spectroscopic Ψ values were modelled by using the Lorentz model, with theoretical Ψ values then obtained. The refractive indices (n) of the glasses were determined by ensuring the best fitting between the theoretical and experimental values of Ψ. The spectroscopic ellipsometry (SE) spectra of all glasses in the wavelength range of 300–900 nm are shown in Fig. 3.

Our study shows that the fitting between the theoretical model and the experimental data is extremely fine. The MSE (mean square error) values for all the glasses are 0.01, 0.02, 0.04, 0.03, 0.03, 0.04, respectively. The refractive index (n) spectra of the glasses are given in Fig. 4.

In Fig. 4, it can be seen that changes in the refractive indices of the glasses at long wavelengths are almost constant and occur in a similar form. The refractive index values of the glasses decrease with a corresponding increase in wavelength. Black glass (CoO incorporated) and transition metal doped glasses have higher refractive index values than P1 (base glass). The refractive index values of base

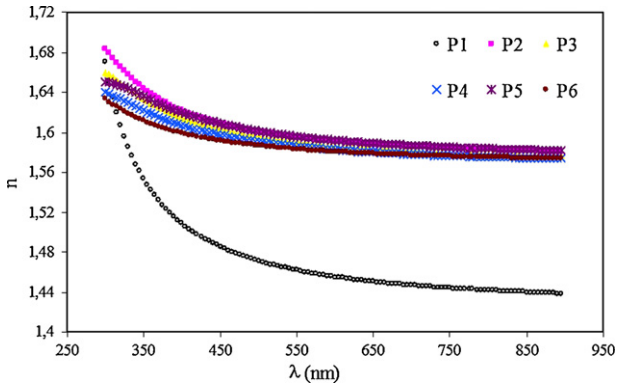

Fig. 4. Refractive index (n) spectra of glasses.

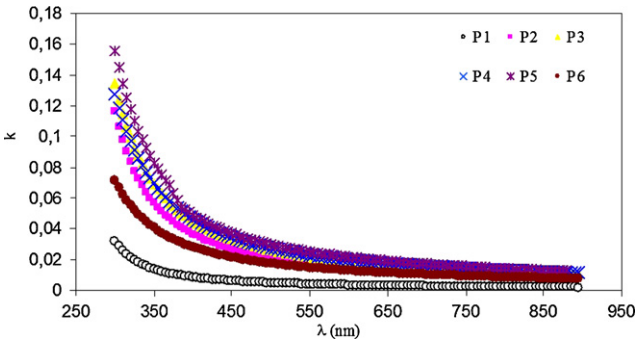

Fig. 5. Extinction coefficient (k) spectra of all glasses.

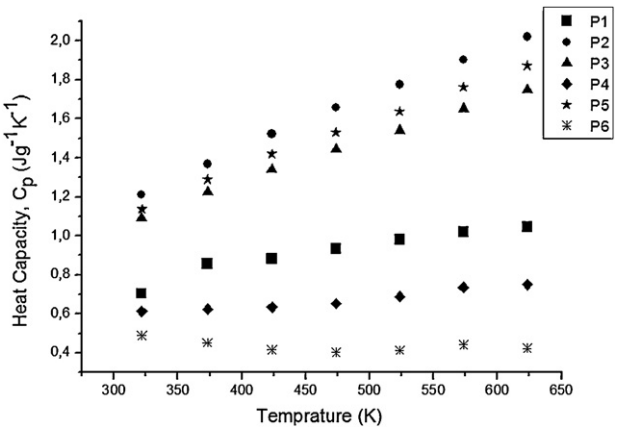

Fig. 6. Specific heat values of glasses as a function of temperature.

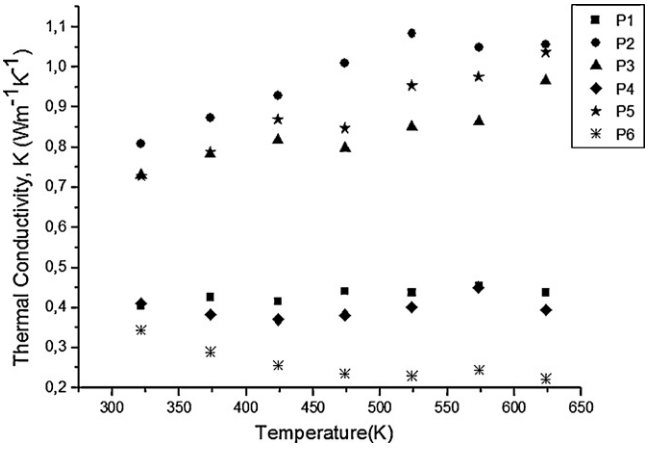

Fig. 7. The calculated thermal conductivities of glasses as a function of temperature.

glass exhibit a noticeable variation in the UV region (~1.68–1.50). However, this variation is smaller than is detected in other glasses (~1.68–1.60). A comparison of the values of the average refractive indices for all glasses is given in Table 2. When we compare the average refractive index values of blank glass (P2), we can observe a decrease in the values caused by both V_2O_5 and CuO doping. If further doping continues, the n values also continue to decrease. Since the values are so close to each other, it is really quite difficult to make any comments with regard to the dopant type. Moreover, it is clear that the higher n values seen in CoO incorporated and transition metal doped glasses, when compared with P1 glass, are due to CoO content. The different density values (Table 2) of different glasses probably also causes the observed variation in n values.

Fig. 5 shows the extinction coefficient spectra of all the glasses. It can be seen that CoO incorporation and transition metal doping processes caused increased absorption values when compared to base glass P1.

3.2. Thermal investigations

The thermal conductivity (K) can be found from the thermal diffusivity (D_T) and specific heat (C_p) measurements through the formula:

$$K = D_T \rho C_p, \quad (1)$$

where ρ is the density of the glass. It is determined by the Archimedes principle, using ethanol as an immersion liquid (density = 0.789 g/cm^3 at room temperature). The densities of all samples are listed in Table 2. As it can be understood from the table, while P1 is the glass with lowest density, P6 is the glass with highest density. As the amount of doping to the glass increased, the density also increased. CuO doping demonstrated a greater increase in the density of the glass than V_2O_5 doping.

The values of the thermal diffusivity coefficient for all the specimens within the stated temperature range are given in Table 3, and the graph of specific heat relative to temperature is given in Fig. 6. The thermal diffusivity coefficient increases with an increase in the temperature. The doped glasses had higher thermal diffusivity values upon measurement.

As can be seen in Fig. 6, the specific heat values of glasses, with the exception of P6, increase with rising temperature. The exception to the rule is P6 glass whose C_p value is not greatly affected by changes in temperature. While the glass with the lowest heat capacity value is P6 glass; the glass with the highest heat capacity is P2 glass.

As is shown in Table 3 and Fig. 6, the thermal conductivity of all glasses was calculated with Eq. (1) and these results are shown in Fig. 7. As can be seen from Fig. 7, with an increase in temperature, the thermal conductivity values of P1 and P4 remain almost constant, while that of P6 displays a slight decrease, and those of P2, P5, and P3 have a noticeable increase. The glass with the highest thermal conductivity is P2 while the glass with the lowest ther-

Table 3
Thermal diffusivity values of all glasses.

P1		P2		P3		P4		P5		P6	
$T(K)$	$D_T \times 10^{-6}$ (m^2 s^{-1})	$T(K)$	$D_T \times 10^{-6}$ (m^2 s^{-1})	$T(K)$	$D_T \times 10^{-6}$ (m^2 s^{-1})	$T(K)$	$D_T \times 10^{-6}$ (m^2 s^{-1})	$T(K)$	$D_T \times 10^{-6}$ (m^2 s^{-1})	$T(K)$	$D_T \times 10^{-6}$ (m^2 s^{-1})
321.75	0.22	321.75	0.23	321.75	0.23	321.85	0.23	321.95	0.22	321.85	0.24
373.35	0.19	373.35	0.22	373.25	0.22	373.35	0.21	373.35	0.21	373.35	0.22
423.75	0.18	423.65	0.21	423.65	0.21	423.75	0.2	423.65	0.21	423.75	0.21
473.75	0.18	473.75	0.21	473.75	0.19	473.75	0.2	473.65	0.19	473.75	0.2
523.65	0.17	523.75	0.21	523.65	0.19	523.65	0.2	523.75	0.2	523.65	0.19
573.55	0.17	573.65	0.19	573.55	0.18	573.45	0.21	573.35	0.19	573.55	0.19
623.55	0.16	623.55	0.18	623.25	0.19	623.45	0.18	623.35	0.19	623.45	0.18

mal conductivity is P6. CuO and V_2O_5 doping causes the thermal conductivity of blank (P2) glass to decrease. There is not a linear variation between the doping amount and thermal conductivity. However, it is clear that high doping rates force thermal conductivity values to decrease for both types of dopants, namely V_2O_5 and CuO. CuO doping at 0.5% caused higher thermal conductivity values than V_2O_5.

4. Conclusions

In this study, the effect of transition metal ions such as V_2O_5 and CuO on the optical and thermal characteristics of black glass has been investigated.

It was determined that the incorporation of CoO at 20% almost destroys absorption in the visible region from the absorption spectra. V_2O_5 doped glasses absorb the UV region and CuO doped glasses absorb the NIR region. Thus, since the absorption spectra at base glass are considerably affected by doping, we believe that it is a strong contender for use in future applications in solar collectors. Furthermore, the absorption edge shifted to longer wavelengths as the concentration of V_2O_5 and CuO increased. Doping by both V_2O_5 and CuO caused the direct and indirect band gap values to decrease. The values of the refractive index for all glasses decrease as the wavelength increases. Refractive indices at 590 nm varied from 1.456 to 1.591. The glass with the lowest refractive index is P1 and the one with the highest refractive index is P2. It is our opinion that an excess of unbounded oxygen in the P2 glass caused the polarization to increase, which in turn increased the refractive index. The incorporation of CoO reduced the number of unbounded oxygen in the P2 glass and this probably, in turn, decreased the refractive index value.

The thermal conductivity coefficients of all the glasses were calculated by considering the heat capacity, thermal diffusivity coefficient, and density values. While the thermal conductivities of P1 and P4 glasses remain almost constant depending on the temperature, the thermal conductivities of P2, P3 and P5 glasses increased with a rise in temperature, whereas the thermal conductivity of P6 glass decreased with an increase in temperature. By increasing the temperature, the number of phonon–phonon collisions increases, and thus, the mean free path of the phonons decreases. This then leads to a decrease in thermal conductivity. In general, phonon–phonon scattering and phonon–impurity scatterings are dominant mechanisms in thermal conductivity [34]. In our measurements, P6 glass is the specimen which exhibits a decrease in the value of thermal conductivity when temperature increases. The increased doping of CuO (at 1%) commits the role of impurity. Since such a case was not observed in 1% V_2O_5 doped glass, it is thought that V_2O_5 joined to the structure without impurity. Finally, it is our conclusion that CoO incorporation and doping by transition metal ions have a dramatic effect on the properties of sodium–phosphate glasses, and that new and alternative glass materials may be produced economically by this process. We also concluded that CuO doped (at 0.5%) glass is the best candidate for solar collector applications with its improved absorption characteristics and thermal conductivity values.

References

[1] J.A. Wilder, J. Non-Cryst. Solids 38 and 39 (1980) 879.
[2] N.H. Ray, C.J. Lewis, J.N.C. Laycock, W.D. Robinson, Glass Technol. 14 (2) (1973) 50;
N.H. Ray, C.J. Lewis, J.N.C. Laycock, W.D. Robinson, Glass Technol. 14 (2) (1973) 55.
[3] H.A.A. Sidek, I.T. Collier, R.N. Hampton, G.A. Saunders, B. Bridge, Philos. Mag. B 59 (1989) 221.
[4] E. Kordes, R. Nieder, Glastech. Ber. 41 (1968) 41.
[5] P.P. Proulx, G. Cormier, J.A. Capobianco, B. Champagnon, M. Bettinelli, J. Phys. Condens. Matter 6 (1994) 275.
[6] M.J. Weber, J. Non-Cryst. Solids 123 (1990) 208.
[7] B. Kumar, S. Lin, J. Am. Ceram. Soc. 74 (1991) 226.
[8] P. Ducheyne, MRS Bull. 23 (1998) 43.
[9] N.F. Mott, J. Non-Cryst. Solids 1 (1968) 1.
[10] L. Murawski, C.H. Chung, J.D. Mackenzie, J. Non-Cryst. Solids 32 (1979) 91.
[11] J.C. Bazan, J.A. Duffy, M.D. Ingram, M.R. Mallance, Solid State Ionics 86–88 (1996) 497.
[12] G. Jayasinghe, M. Dissanayake, M. Careem, J.-L. Souquet, Solid State Ionics 93 (1996) 291.
[13] H. Hirashima, K. Nishi, T. Yoshida, J. Am. Ceram. Soc. 66 (10) (1983) 7070.
[14] A. Kutub, A.E. Mohamed-Osman, C.A. Horgarth, J. Mater. Sci. 21 (1986) 3517.
[15] C.F. Drake, I.F. Scalan, A. Engel, Phys. Status Solidi 32 (1969) 193.
[16] G.R. Moridi, C.A. Horgarth, Proc. 7th Int. Conf. Amorphous Liq. Semi-cond., 1977, p. 688.
[17] G.R. Moridi, C.A. Horgarth, Int. J. Electron. 44 (3) (1978) 297.
[18] L.E. Bausa, F. Jaque, J.G. Sole, A. Duran, J. Mater. Sci. 23 (6) (1988) 1921.
[19] M. Jamnicky, P. Znasik, D. Tunega, M.D. Ingram, J. Non-Cryst. Solids 185 (1995) 151.
[20] N. Satyanarayana, G. Gorindaraj, A. Karthikeyan, J. Non-Cryst. Solids 136 (1991) 219.
[21] U. Selveraj, K.J. Rao, J. Non-Cryst. Solids 72 (1985) 315.
[22] T. Minami, K. Imazawa, M. Tanaka, J. Non-Cryst. Solids 42 (1980) 469.
[23] S.H. Kim, T. Yoko, J. Am. Ceram. Soc. 78 (1995) 1061.
[24] G.D. Khattak, E.E. Khawaja, L.E. Wenger, D.J. Thompson, M.A. Salim, A.B. Hallak, M.A. Daous, J. Non-Cryst. Solids 194 (1996) 1.
[25] M.A. Chaudhry, M. Altaf, Mater. Lett. 34 (1998) 213–216.
[26] F.M. Nazar, M.A. Ghauri, J. Mater. Sci. 17 (1982) 3653.
[27] S.A. Sıddıqı, R.D. Khan, F.A. Khwaja, S. Naseem, Int. J. Electron. 64 (1988) 661.
[28] R.A. Synowicki, Thin Solid Films 313 (1998) 394–397.
[29] J.N. Hilfiker, N. Singh, T. Tiwald, D. Convey, S.M. Smith, J.H. Baker, H.G. Tompkins, Thin Solid Films 516 (2008) 7979–7989.
[30] F.H. ElBatal, Y.M. Hamdy, S.Y. Marzouk, Mater. Chem. Phys. 112 (2008) 991–1000.
[31] S. Sakka, K. Kamiya, K. Makita, Y. Yamamoto, J. Non-Cryst. Solids 63 (1984) 223.
[32] F.A. Davis, N.F. Mott, Philos. Mag. 22 (1970) 903.
[33] Y.C. Ratnakaram, A. Viswanadha Reddy, J. Non-Cryst. Solids 277 (2000) 142–154.
[34] S. Kim, C. Joung, H. Kim, Y. Lee, H. Ryu, D. Sohn, D. Kim, J. Nucl. Mater. 352 (2006) 151–156.